BIOCHEMISTRY
including biophysical chemistry & molecular biology

Article

pubs.acs.org/biochemistry

Combining Experimental Evidence and Molecular Dynamic Simulations To Understand the Mechanism of Action of the Antimicrobial Octapeptide Jelleine-I

Marcia Perez dos Santos Cabrera,[*,‡,⊥] Gisele Baldissera,[⊥,¶] Laiz da Costa Silva-Gonçalves,[§] Bibiana Monson de Souza,[∥] Karin A. Riske,[§] Mario Sérgio Palma,[∥] José Roberto Ruggiero,[⊥] and Manoel Arcisio-Miranda[§]

[‡]Departamento de Química e Ciências Ambientais, Universidade Estadual Paulista, São José do Rio Preto, São Paulo 15054-000, Brazil

[⊥]Departamento de Física, Universidade Estadual Paulista, São José do Rio Preto, São Paulo 15054-000, Brazil

[§]Departamento de Biofísica, Universidade Federal de São Paulo, São Paulo, São Paulo 04023-062, Brazil

[∥]Centro de Estudos de Insetos Sociais, Universidade Estadual Paulista, Rio Claro, São Paulo 13506-900, Brazil

[¶]Faculdade de Tecnologia de Catanduva, Catanduva, São Paulo 15800-200, Brazil

Supporting Information

ABSTRACT: Jelleines are four naturally occurring peptides that comprise approximately eight or nine C-terminal residues in the sequence of the major royal jelly protein 1 precursor (*Apis mellifera*). The difference between these peptides is limited to one residue in the sequence, but this residue has a significant impact in their efficacy as antimicrobials. In peptide-bilayer experiments, we demonstrated that the lytic, pore-forming activity of Jelleine-I is similar to that of other cationic antimicrobial peptides, which exhibit stronger activity on anionic bilayers. Results from molecular dynamics simulations suggested that the presence of a proline residue at the first position is the underlying reason for the higher efficacy of Jelleine-I compared with the other jelleines. Additionally, simulations suggested that Jelleine-I tends to form aggregates in water and in the presence of mimetic membrane environments. Combined experimental evidence and simulations showed that the protonation of the histidine residue potentiates the interaction with anionic palmitoyl-oleoyl-phosphatidylcholine/palmitoyl-oleoyl-phosphatidylglycerol (POPC/POPG) (70:30) bilayers and reduces the free energy barrier for water passage. The interaction is driven by electrostatic interactions with the headgroup region of the bilayer with some disturbance of the acyl chain region. Our findings point to a mechanism of action by which aggregated Jelleine-I accumulates on the headgroup region of the membrane. Remaining in this form, Jelleine-I could exert pressure to accommodate its polar and nonpolar residues on the amphiphilic environment of the membrane. This pressure could open pores or defects, could disturb the bilayer continuity, and leakage would be observed. The agreement between experimental data and simulations in mimetic membranes suggests that this approach may be a valuable tool to the understanding of the molecular mechanisms of action.

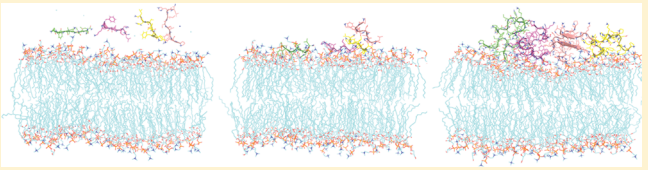

Natural products have been the main source or guide to the development of new antibiotic substances.[1] Insect secretions appear to be rich reservoirs of antimicrobial peptides with therapeutic potential. In royal jelly, four short chain peptides were identified, and their biological activity was characterized. Jelleine-I (JI, PFKISIHL), Jelleine-II (JII, TPFKISIHL), and Jelleine-III (JIII, EPFKISIHL) are active against Gram-positive and Gram-negative bacteria, mostly in decreasing order in terms of their efficiency as antimicrobials (JI > JII ≫ JIII). For instance, against *Staphylococcus aureus* or *Pseudomonas aeruginosa*, minimum inhibitory concentration (MIC) values are 10.5 μM for JI, 14.2 μM for JII, and 27.7 μM for JIII. JI and JII are equally active against the yeast *Candida albicans*, while JIII is not active. Jelleine-IV (JIV, TPFKISIH) has no antimicrobial effects in relation to the tested strains. The four peptides show poor hemolytic (less than 10%) and mast cell degranulation activities (less than 3%).[2,3]

From a structural standpoint, jelleines are hydrophobic peptides whose sequences bear no similarity to other antimicrobial peptides from honeybees.[2] They contain one proline and one histidine residue. The protonation state of histidine is dependent on the environmental pH and may modulate the activity of the peptide.[4,5] The pH-dependent activity was not studied in many cases, but it seems to be an important factor since several organs and disease states have or develop an acidic environment.[6,7] Mason and co-workers

Received: March 24, 2014
Revised: June 25, 2014
Published: June 27, 2014

(2009)[8] demonstrated that longer chain length peptides that are cationic, amphipathic, and rich in histidine residues have enhanced lytic and antibiotic properties. Moreover, these peptides can induce punctate ruptures in the membrane, forming pores, while the rest of the membrane is left intact. Such effects are triggered by acidic pH. Also, Makovitzki et al. (2009)[9] mutated lysine residues in tumoricidal peptides to histidine residues. The histidine residues become protonated by the acidic environment produced in solid tumors, thus triggering the lytic activity of the peptides in a targeted manner. This substitution also reduced the systemic toxicity of the peptides compared with peptides containing lysine residues. In common with proline-rich antimicrobial peptides, jelleines show selective activity toward Gram-negative bacteria and low hemolytic activity.[2,10]

In this study, by combining experimental data related to the activity of jelleines on model membranes with molecular dynamics simulations (MD), we have addressed the following questions about their modes of action: (1) Using MD, we prospected for the molecular reason for the enhanced antibacterial activity of JI in relation to the other jelleines. (2) We analyzed the possibility of synergic activity between JI and each of the other jelleines. (3) The influence of the protonated state of a single histidine in the JI structure was measured and correlated to simulation results. (4) The membrane selectivity among different lipid compositions mimicking bacterial (PC/PG 70:30),[11,12] *C. albicans* (PC/PS/Erg 40:40:20),[13] and mammalian erythrocytes (PC/SPH/Chol 40:40:20)[12,14] was considered, and the effects of JI on lipid bilayer characteristics were experimentally and theoretically evaluated.

The agreement between experimental data and simulations in mimetic membranes suggests that this approach may be a valuable tool to the understanding of molecular mechanisms of action.

EXPERIMENTAL PROCEDURES

Materials. Avanti Polar Lipids (Alabaster, AL) supplied the phospholipids egg L-α-phosphatidylcholine (PC), egg L-α-phosphatidylglycerol sodium salt (PG), 1-palmitoyl-2-oleoyl-*sn*-glycero-3-phosphocholine (POPC), 1-palmitoyl-2-oleoyl-*sn*-glycero-3-phospho-(1′-*rac*-glycerol) sodium salt (POPG), and 1,2-dioleoyl-*sn*-glycero-3-phosphocholine (DOPC). Sigma-Aldrich Co. (S. Louis, MO) supplied cholesterol (Chol), ergosterol (Erg), bovine brain sphingomyelin (SPH), bovine brain L-α-phosphatidyl-L-serine (PS), sodium dodecyl sulfate (SDS), 5,6-carboxyfluorescein (CF), and diphenylhexatriene (DPH). All materials were used as supplied. Other chemicals were of high quality analytical grade.

Peptide Synthesis, Purification and Mass Spectrometry Analyses. Peptides were synthesized by stepwise manual solid-phase synthesis using the *N*-9-fluorophenylmethoxycarbonyl (Fmoc) strategy.[15] The crude product was purified by reverse-phase HPLC and the homogeneity and sequence were assessed by analytical HPLC and mass spectrometry (ESI-MS). Samples were analyzed on an ion trap/ToF mass spectrometer (model IT-ToF, Shimadzu, Japan), equipped with a standard electrospray probe (see Supporting Information for further details).

Jelleine stock solutions (100 μM) were prepared in quartz bidistilled water and kept under refrigeration.

Dye Leakage. CF leakage experiments were performed using an ISS PC1 spectrofluorometer (ISS, Urbana−Champaign, IL, USA) at 25 °C, with large unilamellar vesicles (LUVs) of the following lipid composition: 70:30 PC/PG (mimicking a general bacterial membrane),[11,12] 40:40:20 PC/PS/Erg (*C. albicans* mimetic membrane),[13] and 40:40:20 PC/SPH/Chol (mimicking an average red blood cell;[12,14] see Supporting Information for LUV preparation). An aliquot of CF-filled vesicles was added to 10 mM Tris−HCl buffer, containing 1 mM Na_2EDTA and 150 mM NaCl, pH 7.4, in a 1 cm quartz cuvette to give a final lipid concentration of 100 μM. Into the magnetically stirred vesicle suspension, an aliquot of the peptide stock solution was added to obtain the desired final concentration. The fluorescence intensity of CF was monitored at 520 nm wavelength with a 0.5 nm slit width (excited at 490 nm wavelength with 1.0 nm slit width). The percentage of CF release was calculated using the following equation: % leakage = $100(F - F_0)/(F_{100} - F_0)$, where F is the observed fluorescence intensity and F_0 and F_{100} correspond, respectively, to the fluorescence intensities in the absence of peptides and that at 100% leakage, as determined by the addition of 20 μL of 10% Triton X-100 solution. F_{100} has been corrected for the corresponding dilution factor.

Optical Microscopy Observation of Giant Unilamellar Vesicles (GUVs). An aliquot of the vesicle suspension (see Supporting Information for GUV preparation) was diluted 7-fold into a 0.2 M glucose solution. The differences in density and refractive index between sucrose inside and glucose outside the vesicles provide better contrast for observation under the phase contrast microscope and also stabilize GUVs by gravity. To avoid osmotic pressure effects, the osmolarities of the sucrose and glucose solutions were checked with an osmometer (Osmomat Gonotec 030, Berlin, Germany) and carefully matched. In each experiment, 5 μL of POPC/POPG (70:30) GUV suspension was added, without stirring, into the observation chamber, which already contained different volumes of JI stock solution (prepared in 0.2 M glucose) and 0.2 M glucose solution to complete 95 μL. Vesicles were observed under 40× or 63× phase contrast objectives installed in a Zeiss Axiovert 200 microscope (Carl Zeiss, Jena, Germany) equipped with a Zeiss AxioCam HSm digital camera. Images were captured starting immediately after the injection of JI using Zeiss Axiovision software. Representative vesicles were then brought into focus and followed.

Planar Lipid Bilayer Preparation, Electrophysiology Measurements, and Analysis. Planar lipid bilayers were formed from a mixture of DOPC/POPG (70:30) dissolved in *n*-decane (25 mg/mL), according to the method of Mueller et al. (1963).[16] To form a membrane, the lipid solution was spread across a hole (~0.2 mm for single channel records or ~0.7 mm for macroscopic records) formed in a polyethylene film of 100 μm thickness fixed in an acrylic chamber, defining two 5 mL compartments (cis and trans). Both compartments were filled with buffer solution composed of 10 mM Tris and 150 mM KCl, pH 7.4, or 10 mM $C_6H_8O_7$, 10 mM Na_2HPO_4, 150 mM KCl, pH 5.5, for macroscopic records. For single channel records, the same buffers were used, but the KCl concentration was raised to 1 M. Electrical access to the bath was through a pair of Ag/AgCl electrodes. The front compartment (cis) was held at ground (0 mV) and the posterior compartment (trans) was clamped at chosen potential by a patch-clamp amplifier (PC-One, Dagan Corporation, Minnesota, USA), configured in voltage-clamp mode. JI, at a final concentration of 5 μM, was added into the cis compartment, which was stirred for 2 min. The macroscopic protocol consisted of the application of square pulses with frequency of 10 mHz and amplitude of 10 mV p-p through the arbitrary waveform generator (model 33521A, Agilent Technologies, California, USA). All experiments were carried out at

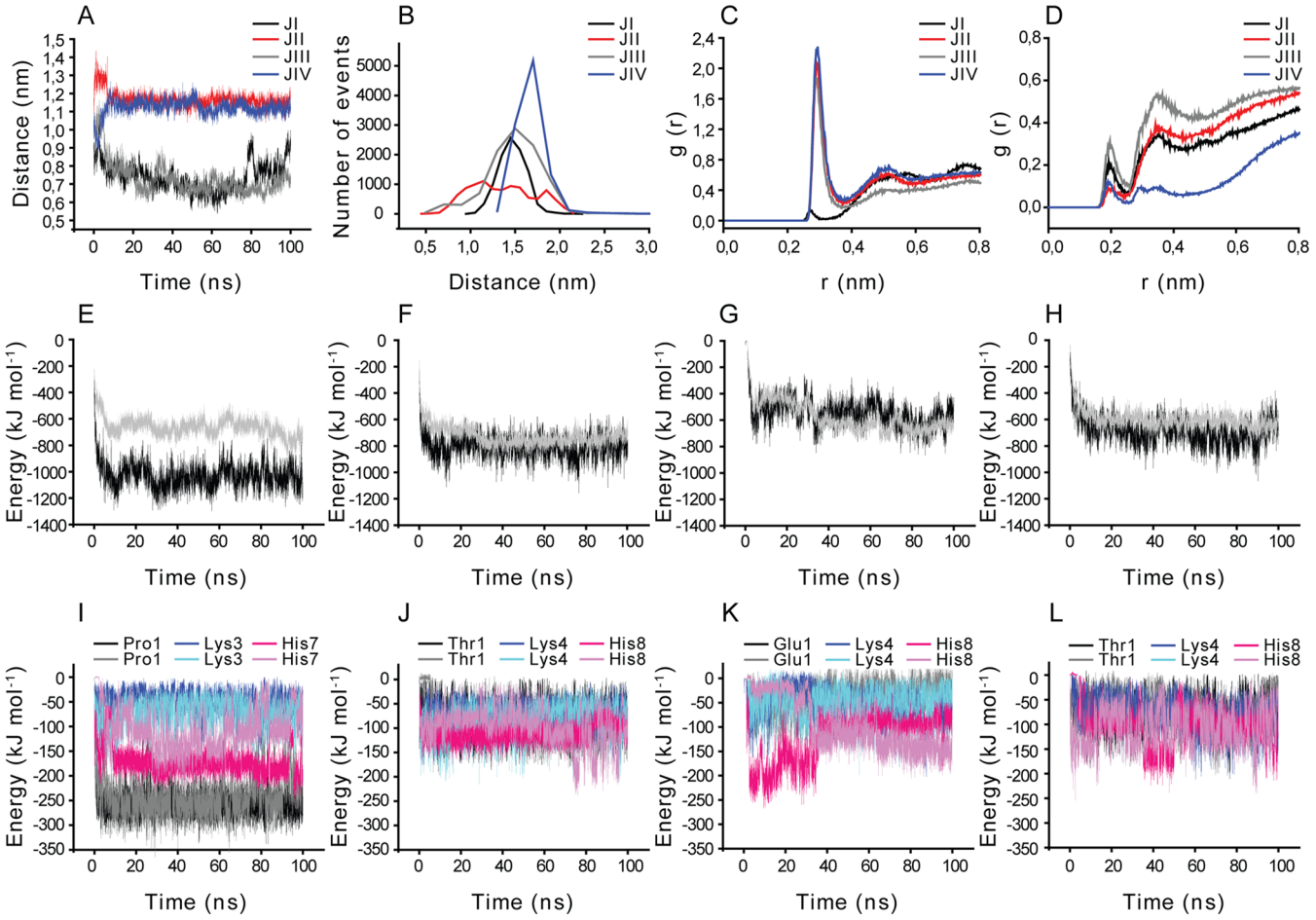

Figure 1. MD simulations of jelleines-I–IV in SDS micelle. (A) Distance between the centers of mass of peptide molecules. (B) Histogram of the most probable distance of peptide pairs to the center of mass of the SDS micelle. (C, D) Solvation profiles of N- and C-terminal residues, respectively. (E–H) Coulomb (black) and Lennard-Jones (gray) contributions to the interaction energy between peptides and the SDS micelle: (E) JI, (F) JII, (G) JIII, and (H) JIV. (I–L) Coulomb contribution to the interaction energy between charged or polar amino acids and the micelle: (I) JI, (J) JII, (K) JIII, and (L) JIV.

room temperature (23–25 °C). The single channel records and the measured macroscopic activity were analyzed with the Clampfit software (Molecular Devices, California, USA). The statistical analyses were performed with GraphPad Prism 5.0 software (GraphPad Software, California, USA). The membrane conductance (G_m) was determined as $G_m = I_m/V_{clamp}$; where I_m is the transmembrane current and V_{clamp} is the applied potential.

ζ-Potential Determination and Size Measurements. The binding of JI was assessed through the changes in ζ-potential of the PC/PG 70:30 and PC/PS/Erg 40:40:20 LUVs with a Nano Zetasizer ZS90 (Malvern Instruments, Worcestershire, U.K.). Aliquots of vesicle suspension to give a final concentration of 100 μM were added to peptide solutions in buffer whose concentration ranged from 0 to 27.5 μM, pH 5.5, in 1.5 mL plastic vials. Each preparation was equilibrated for 30 min at 25 °C. Next, each preparation was transferred to a disposable cuvette for size evaluation and, afterward, to a DTS1060 cell (Malvern Instruments) for ζ-potential measurement.

Circular Dichroism (CD) Measurements. CD spectra were acquired in buffer containing 20 μM peptide and 8 mM SDS solution. CD spectra were recorded from 260 to 200 nm with a Jasco-710 spectropolarimeter (JASCO International Co. Ltd., Tokyo, Japan). Spectra were acquired at 25 °C using a 0.5 cm cell path length, averaged over eight scans, at a scan speed of 20 nm/min, bandwidth of 1.0 nm, 0.5 s response, and 0.1 nm resolution. Following baseline correction, the observed ellipticity (θ (mdeg)) was converted to mean residue ellipticity ([Θ] (deg cm^2/dmol)) using the relationship $[\Theta] = 100\theta/(lcn)$, where l is the path length in centimeters, c is peptide millimolar concentration, and n the number of peptide bonds.

Fluorescence Anisotropy of the Probe DPH. Aliquots of vesicle suspension (PC/PG 70:30 containing DPH) to give a final concentration of 50 μM were added to peptide solutions in buffer with concentrations ranging from 0 to 12.5 μM, pH 5.5, in disposable cuvettes. Each preparation was equilibrated for 3 h at 25 °C, protected from light. Steady state fluorescence anisotropy, r, was measured using the above-mentioned spectrofluorometer, at 25 °C, monitored at 450 nm wavelength with 2.0 nm slit width (excited at 360 nm wavelength with 2.0 nm slit width), equipped with Glan-Thompson polarizers in the routine for polarization. R-values were automatically calculated by the software provided by ISS.[17]

Molecular Dynamics (MD) Simulations. Simulations were performed in boxes of various sizes to accommodate the different systems and with enough water molecules to guarantee the water density. The systems studied are a preformed SDS micelle in a cubic box, consisting of 65 SDS molecules, approximately 12000 water molecules, and enough counterions to neutralize the system and POPC/POPG (70:30 molar ratio) membranes consisting of 90 POPC and 38 POPG molecules (considering the

dx.doi.org/10.1021/bi5003585 | Biochemistry 2014, 53, 4857–4868

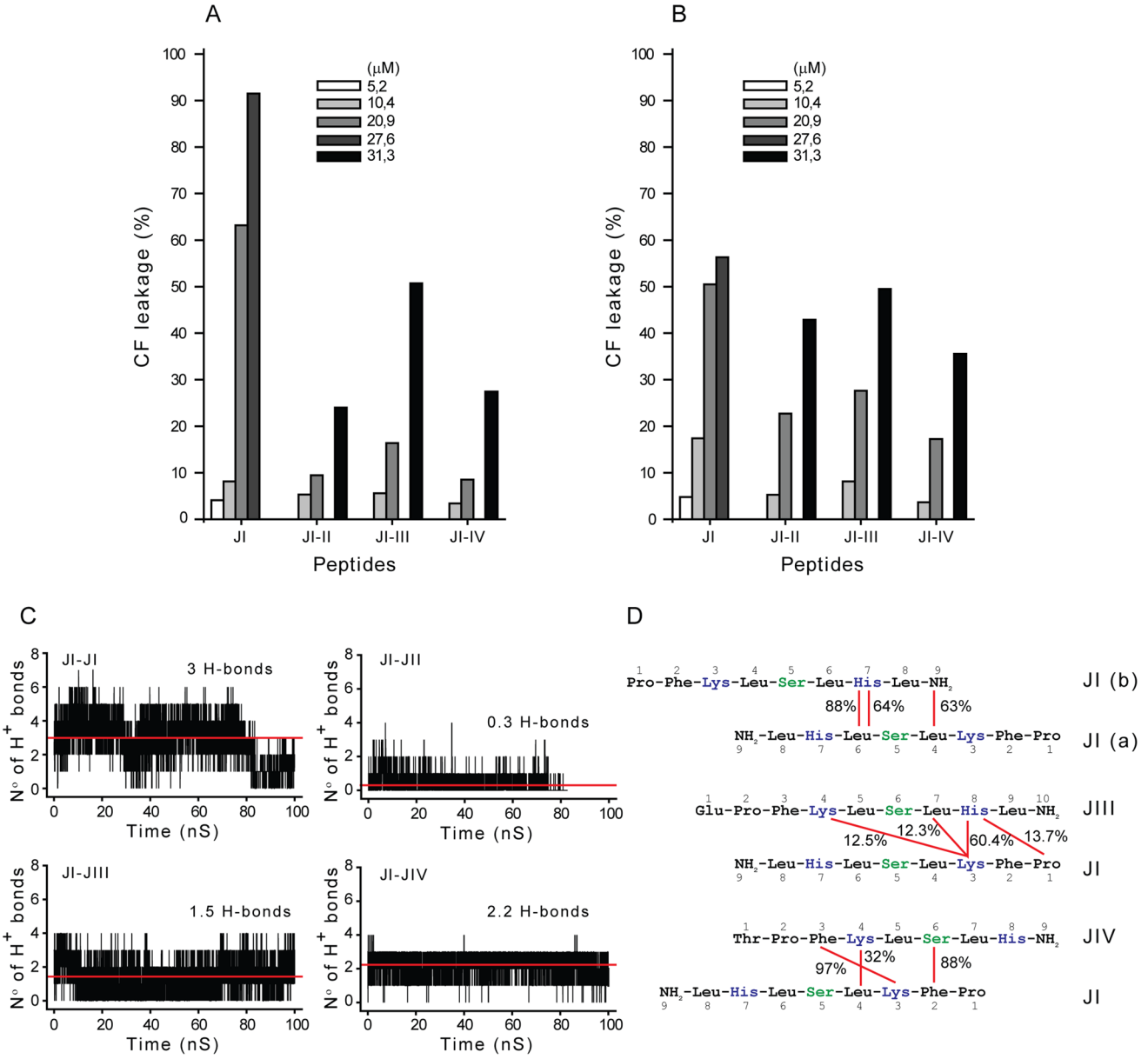

Figure 2. Effects of combined jelleines in 1:1 mixtures of JI–JII, JI–JIII, and JI–JIV compared with JI. CF leakage after 10 min from 100 μM LUVs of PC/PG 70:30 (A) and PC/PS/Erg 40:40:20 (B) at different peptide concentrations, at pH 7.4 and 25 °C. (C) Number of hydrogen bonds formed between peptide pairs in the presence of a SDS micelle. Red lines represent the average values for hydrogen bonds. (D) Representation of the longer lasting hydrogen bonds between peptide pairs as a % of the simulation time.

two possible chiralities of POPG), 38 Na^+ ions and approximately 4500 water molecules, all of them randomly placed. We conducted seven separate simulations with the SDS micelle present in which there were two peptide molecules each. Four simulations included the four pure jelleines individually, and the other three simulations contained mixtures of JI and one of the other jelleines, For the systems with the POPC/POPG 70:30 membrane, we carried out five independent simulations, one to obtain the pure membrane by self-assembly (also used as reference), two with four peptides, simulating pH 5.5 and pH 7.0, and afterward another two were run for the same pH conditions but with 16 peptide molecules. The different pHs in the simulations was represented through the histidine residue protonation. At pH 5.5, all histidine residues were protonated, while at pH 7.0, 50 percent of the histidine residues in peptides were protonated.

Simulation Conditions and Evaluation. All simulations were performed and analyzed using the Gromacs 4.0.7 package,[18,19] with an NPT ensemble and temperature set at 300 K. The following GROMOS force field sets were used according to the system to be simulated: 43A1 (simulations in water),[20] 45A3 (simulations in SDS),[21,22] and 53A6 (simulations with lipid bilayer).[23] These three force field sets are equivalent for the atoms of the peptides.[24]

RESULTS AND DISCUSSION

Investigating the Role of Sequence Differences among Jelleines. Systematic studies of amino acid substitutions in jelleines have recently been carried out and the resulting literature speaks to the impact of subtle sequence variations on Jelleine antimicrobial activity.[25−28] Because the various Jelleine sequences differ by only one residue, the structural detail

dx.doi.org/10.1021/bi5003585 | Biochemistry 2014, 53, 4857−4868

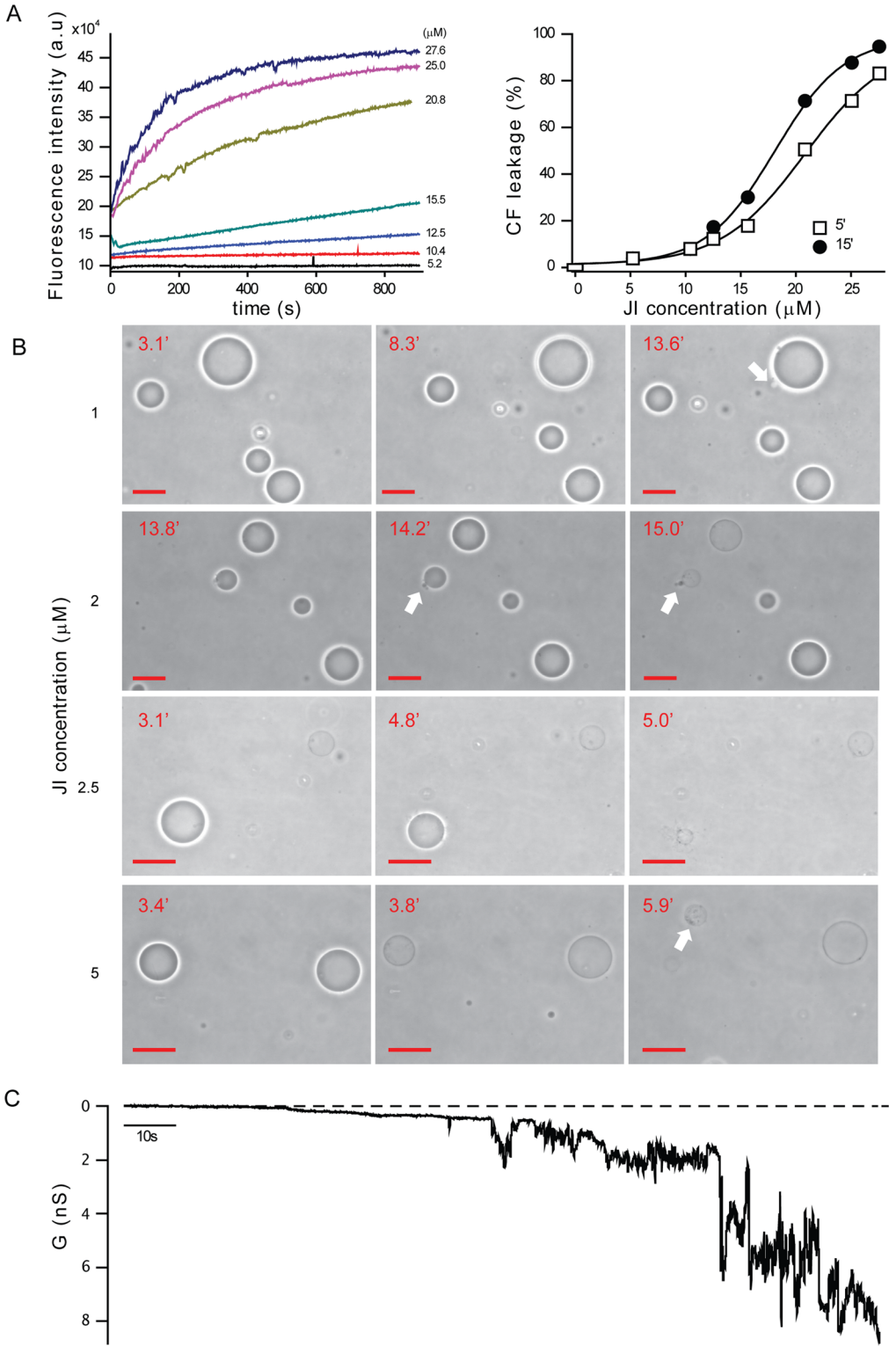

Figure 3. Permeabilizing effect of Jelleine-I in different membrane mimetic systems. (A) Kinetics of CF leakage from 100 μM PC/PG 70:30 LUVs (left) and respective sigmoid dose−response curves, fitted according to the Boltzmann sigmoid model, at 5 and 15 min contact time (right), obtained at 25 °C, pH 7.4. (B) Phase contrast snapshots of the lytic effects of JI on GUVs made of POPC/POPG 70:30, at room temperature (23−25 °C). The time is shown from the start of the GUV dilution. The scale bars correspond to 20 μm. (C) The time course of insertion of JI (5 μM) into DOPC/POPG 70:30 planar lipid bilayer at −50 mV, in 150 mM KCl, 10 mM Tris, pH 7.4, at room temperature. The dashed line is the zeroed-conductance level.

provided by MD simulations can offer molecular explanations for the differences in biological activity of these peptides.

Simulations of jelleines-I−IV were initially carried out in water with two equal and separated 100% ideal α-helical configuration peptides. Simulations for 200 ns indicated that jelleines rapidly lose this initial conformation, forming long lasting hydrogen bonds between molecules, mostly in a random-coil conformation (Supporting Information, Figure 1).

dx.doi.org/10.1021/bi5003585 | *Biochemistry* 2014, 53, 4857−4868

Next, to investigate the interaction of each Jelleine with a model membrane system, four independent MD simulations were performed in the presence of an SDS micelle, which is a mimetic system of the anionic character of bacterial membranes. Figure 1 describes the main features of peptide−peptide interactions and peptide−membrane interactions as distances, solvation, and interaction energy. The distance between the Jelleine molecules as a function of simulation time and the most probable distance between peptides and the micelle center of mass were calculated, allowing us to consider the importance of peptide−peptide interactions for peptide−membrane contacts. We observed four main features: (1) The pair of molecules of JI and the pair of molecules of JIII are closer to each other than the two molecules of JII and the two molecules of JIV (Figure 1A). (2) JI and JIII assume an equivalent position, closest to the micelle's center. JIV is the most distant, and JII assumes variable positions (Figure 1B). (3) Considering the first solvation layer, the solvation profile of the JI N-terminus shows significant absence of water compared with the other jelleines (Figure 1C). The solvation profiles of C-termini are similar for the four peptides (Figure 1D). (4) Coulomb and Lennard-Jones contributions to the energy of interaction between peptides and the micelle indicate that the electrostatic component is more relevant for JI (Figure 1E−H). To further investigate the difference in the Coulombic contribution, the interaction energy between charged residues and the SDS micelle was analyzed (Figures 1I−L). Comparing the first residue of each peptide, we verified that the Pro1 residue in JI has greater interaction energy than the other ones. Also, it seems that Pro1 can exert some sort of favorable influence for the interaction of the His7 residue. This could concern the secondary structure of JI, and the effect is not seen in the other jelleines. Hansen (2010)[25] showed improvement of the antibacterial activity when substituting Pro1 with Ala together with substitutions of Ser5 with Ile. The hemolytic activity of these mutants was reduced, which suggests that the effect of the substitutions was likely mediated through alterations in secondary structure and not due to increasing hydrophobicity. These results speak to the importance of the N-terminal residues in the antimicrobial activity of jelleines.[25,26] The presence of a Thr1 residue in JII and JIV and Glu1 in JIII attracts more water molecules to the N-terminus and might be the cause of their decreased interaction with the SDS micelle.

Effects of Combined Jelleines. The biological significance of many homologous sequences within one species is far from being well understood, but in a few cases, synergy has already been demonstrated among related peptides.[29,30] Considering that the above results suggest that the peptide−membrane contacts could be influenced by the peptide−peptide interactions and that Coulombic contribution to the interaction energy is more significant than Lennard-Jones, we tested whether JII, JIII, or JIV could synergistically affect the activity of JI. To this end, we compared the extent of CF leakage from LUVs induced by JI and mixtures at a 1:1 molar ratio of JI−JII, JI−JIII, and JI−JIV. Two different lipid compositions were used: PC/PG 70:30 (Figure 2A) and PC/PS/Erg 40:40:20 (Figure 2B). As shown in Figure 2, the mixtures do not show positive synergy either in PC/PG or in PC/PS/Erg vesicles, since the percentage of CF leakage of the peptide mixtures at around 20 μM are comparable to the leakage caused by 10 μM of JI alone.

MD analysis of the interactions between the different mixtures of jelleines (i.e., JI−JI, JI−JII, JI−JIII, and JI−JIV) revealed that association between peptide molecules can occur (Figure 2C). JI−JIII and JI−JIV associate through a smaller number of hydrogen bonds than JI−JI. Figure 2D shows which hydrogen bonds are more stable throughout the simulation time. For the three mixtures, the chains assume an approximately antiparallel orientation; however, the hydrogen bonds between JI−JI molecules do not require torsion or bending of one chain in relation to the other to form.

Lytic and Pore-Forming Activity of Jelleine-I. The lytic activity of antimicrobial peptides in model membranes serves as an evaluation of the permeability of these membranes and the ability of lytic substances to induce pores or defects. Since JII, JIII, and JIV are poor antimicrobial agents and did not show a relevant lytic activity, we centered our investigations on JI using CF leakage experiments on LUVs, electrical measurements on planar bilayers, and leakage from GUVs. The use of these three systems allows us to exclude the influence of membrane curvature and to observe in real time the permeabilizing activity of JI. Figure 3A (left) presents a set of representative spectra obtained when increasing JI concentrations were added to 100 μM LUVs POPC/POPG 70:30. The dose−response curves show that the peptide concentration that triggers the cooperative lytic process (the first inflection point or threshold peptide to lipid, P/L, concentration ratio) is around 12.5 μM or 0.125 P/L (Figure 3A, right), which is close to the MIC found for this peptide with some bacterial strains in the antimicrobial assays.[2]

When we observe POPC/POPG 70:30 GUVs, the increasing peptide concentration causes the initial sucrose/glucose phase contrast to fade, except at 1 μM (Figure 3B). Starting at 2 μM, JI induces further morphological changes, which are seen as denser regions in the bilayer and suggest lipid accumulation mediated by the presence of peptide molecules; it also indicates the pore-forming activity, which allows the mixing of internal and external sugar contents. Similar events were observed with other peptides.[31]

Likewise, JI induced an exponential increase in the conductance of the DOPC/POPG 70:30 planar lipid bilayers (Figure 3C), suggesting that pore-forming activity was responsible for the lytic activity observed in LUVs and GUVs.

Selectivity in the Membrane Interaction of Jelleine-I. The preferential lytic activity of antimicrobial peptides to anionic or zwitterionic vesicles can be evaluated through their ability to induce CF release in bilayers. JI is more lytic to anionic vesicles (Figure 4). It is a cooperative process more efficient in PC/PS/Erg 40:40:20 LUVs, which exhibit a lower threshold P/L ratio (of 0.075) than was observed in PC/PG 70:30 LUVs (of 0.125). Calculation of Hill coefficients resulted 5.5 and 3.4 in PC/PG and PC/PS/Erg, respectively. The lower threshold P/L ratio found in PC/PS/Erg parallels the lower MIC found for *C. albicans*.[2] Likewise in PC/SPH/Chol 40:40:20 vesicles, JI has low lytic activity, following the tendency of low cytotoxicity shown in hemolysis and mast cell degranulation experiments.[2,26]

The binding of JI to anionic LUVs was assessed through ζ-potential experiments, which also confirm the preferential interaction with PC/PS/Erg 40:40:20 vesicles. Figure 4B shows that increasing the JI concentration increases the initial electrokinetic potential (ζ_0) as a consequence of the peptide binding to the vesicle surface. ζ-Potential changes are more pronounced in PC/PS/Erg than in PC/PG 70:30, being more significant until 10 μM JI concentration and then tending to level off. This peptide concentration is close to the threshold P/L determined in the CF leakage experiments. Vesicle size variation of the same samples was also investigated before ζ-potential measurements. They showed that vesicles size is maintained even at the higher peptide concentrations (Figure 4B).

dx.doi.org/10.1021/bi5003585 | *Biochemistry* 2014, 53, 4857−4868

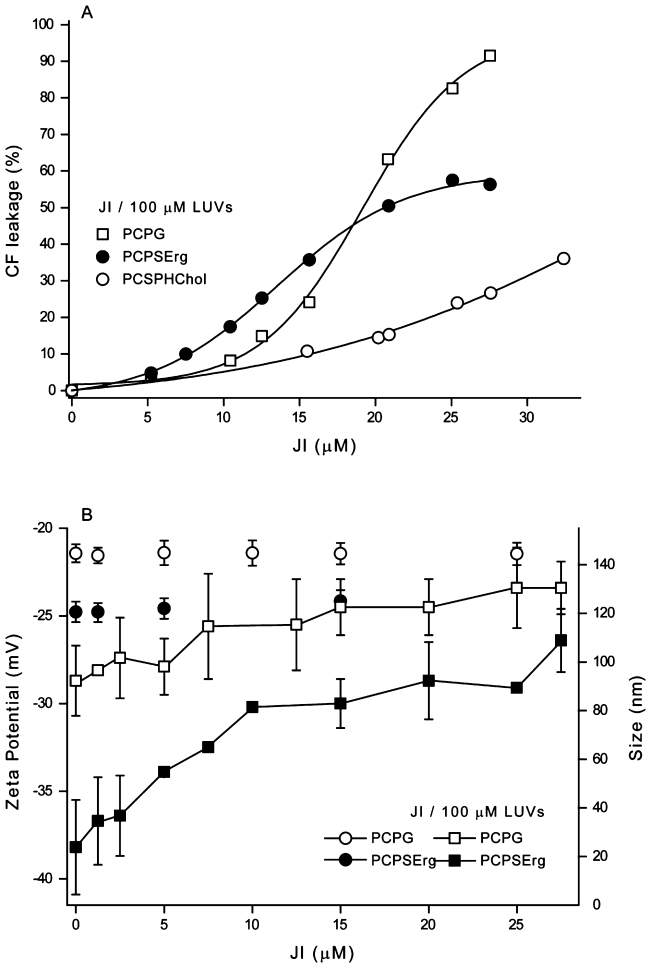

Figure 4. Analysis of the interaction of JI with LUVs of different compositions: PC/PG 70:30, PC/PS/Erg 40:40:20, and PC/SPH/Chol 40:40:20. (A) Dose−response curves obtained from CF leakage experiments after 10 min contact between JI and LUVs, pH 7.4. (B) ζ-Potential isotherms obtained for LUVs, pH 5.5, after 30 min equilibration time (square symbols). ζ-Potential for LUVs in the absence of peptides (ζ_0) is -29 ± 2 mV for PC/PG 70:30 and -38 ± 3 mV for PC/PS/Erg 40:40:20. The same samples were analyzed for size variations (circle symbols).

Protonation of His7 Affects the Pore-Forming Activity of JI. Our initial MD simulations using the SDS micelle helped us to direct the next steps of the investigation to the effects of JI on the lipid bilayer. They indicate that His7 on JI seems to have a more negative energy of interaction with SDS micelles compared with other charged and polar amino acid residues (Figure 1I). We thus hypothesized that the protonated state of His7 could have consequences in the JI structure and/or activity. To test this possibility, we investigated the conformational changes induced by the presence of the SDS micelle environments at pH 5.5 and 7.4. As shown in Supporting Information, Figure 2A, in buffered solution (i.e., without SDS), CD spectra of JI are indicative of random coil conformations with a negative peak around 200 nm under both pH conditions. At pH 5.5 and in the presence of SDS micelles, the spectrum is characteristic of antiparallel β-sheet structure with a negative peak around 217 nm and a positive peak below 200 nm. Due to its short chain length, this structure could be also attributed to interchain hydrogen bonds. At pH 7.4, there is not any characteristic feature. The profiles of secondary structures obtained in the MD simulations for both conditions are also in agreement with a less ordered conformation of JI at pH 7.0 (Supporting Information, Figure 2B) and a significant amount of β-sheet conformation at pH 5.5 (Supporting Information, Figure 2C). The β-sheet conformation has an increased amphipathicity, which is often correlated to increased antimicrobial activity.[32]

Following these experiments, we used electrical measurements on planar lipid bilayers as a finer tool to investigate the effects of the subtle charge difference on pore-forming activity. We first recorded macroscopic current in DOPC/PCPG 70:30 bilayers under pH 5.5 and 7.4. As shown in Figure 5A, when we added a final JI concentration of 5 μM to the *cis*-side of the bilayers and applied square voltage waves, a higher conductance was developed and observed at pH 5.5. The developed current is symmetric at both pHs, indicating that JI does not insert in a preferred orientation into the lipid bilayers.

JI pore-forming activity was further characterized by examining the influence of the environmental pH on conductance in single-channel experiments. Rapid current fluctuations were recorded at both pHs; however, the associated amplitude histogram gave a conductance value of 124 pS at pH 5.5 and 84 pS at pH 7.4 (Figure 5B). The dwell times of the open and the closed states are comparable at both pHs (Figures 5C−F). Nonetheless, the current amplitude vs dwell time of the open state showed that, at pH 5.5, a greater number of higher conductance pores remain open longer (Figures 5G,H) This can account for the higher conductance developed and observed at macroscopic level at pH 5.5.

Next, from MD simulation, we evaluated and compared the Coulomb component of the interaction energy between JI peptides and between JI with POPC/POPG 70:30 bilayer at different histidine protonation states. Simulations for each protonation state ran for 400 ns with four JI molecules in random coil configurations, starting randomly placed in the aqueous environment (approximately at 1.5 nm from the bilayer surface). Figure 6 points to the differences between pH 5.5 and 7.0 obtained during the last 50 ns of the simulations. At pH 5.5, the interaction energy of JI with the bilayer is more favorable, while at pH 7.0, the JI−JI interaction energy is more favorable. These findings are in agreement with the differences observed in the single channel experiments (Figure 5).

Among electrostatic interactions, salt bridges and hydrogen bonds between charged and polar residues were searched. They could differentiate the protonation states under pH 5.5 or 7.0 (Table 1 in Supporting Information). The main findings are (1) JI shows most electrostatic contacts with PC and (2) JI at pH 5.5 significantly increases the number of hydrogen bonds of lipids with water and the number of salt bridges between Pro1 and Lys3 with lipids. Altogether, at lower protonation state, corresponding to pH 7.0, there are 53% and 80% reduction in the total amount of salt bridges of the peptides with POPC and POPG, respectively, and a 64% reduction in the number of hydrogen bonds with POPG.

We had previously seen from the CF leakage experiments that the threshold P/L ratio in PC/PG 70:30 was 1:8 (0.125). To evaluate this condition, four assemblies of four JI molecules as obtained from simulations in water were placed separately and randomly parallel to the bilayer surface. At the end of the simulation, peptides retained the aggregated distribution and anchored at the phospholipids headgroup region. When peptides are in the aggregated form, the interaction occurs with some JI molecules inserted in the lipid bilayer and others more exposed to the solvent. The free energy barrier ($\Delta G(x)$) to water crossing

dx.doi.org/10.1021/bi5003585 | *Biochemistry* 2014, 53, 4857−4868

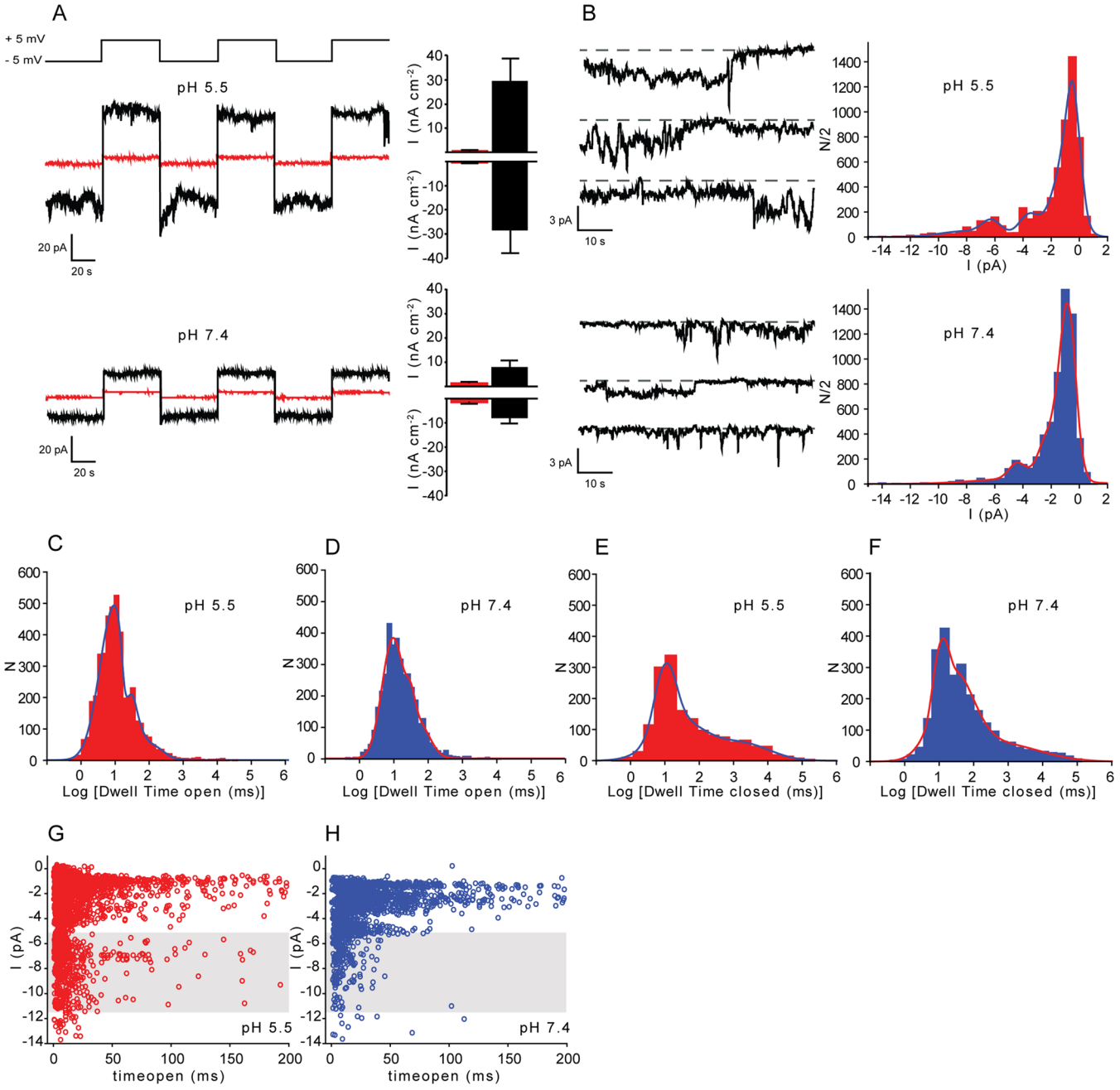

Figure 5. Electrical activity of JI in DOPC/POPG 70:30 bilayers. (A) Macroscopic current−voltage activity. (top) Shows the pulse protocol (square waves with 10 mV p-p amplitude at 10 mHz frequency). (left) Representative current traces obtained before (red) and after (black) the addition of 5 μM of JI at pH 5.5 and at pH 7.4. (right) Correspondent average current values obtained before (red) and after (black) the addition of 5 μM peptide. (B) Representative current traces of JI pore-forming activity at an applied voltage of −50 mV. Dashed lines denote the closed conductive levels. (right) Current amplitude histograms of JI pore-forming activity at pH 5.5 (red) and at pH 7.4 (blue). JI was added to the *cis* compartment at final concentration of 5 μM. (C, D) Corresponding dwell time histograms of the open state. (E, F) Corresponding dwell time histograms of the closed state. (G, H) Relationship between current and open state time of JI pore-forming activity at both pHs.

the bilayer was calculated as $\Delta G(x) = -kT \ln(\rho/1000)$, where k is the Boltzmann constant, T is temperature (K), and ρ is the water density along the normal to the bilayer surface (x), which is the average of 5000 frames over the last 50 ns of the simulation. For the POPC/POPG 70:30 bilayer in the absence of peptides, $\Delta G(x)$ maximum is 40 kJ mol^{-1}, and in simulations with peptides, $\Delta G(x)$ at pH 7.0 and 5.5 are, respectively, 35 and 32 kJ mol^{-1}. This difference between pH conditions is equivalent to 1.2kT (Figure 7A). Figure 7B shows that some water molecules did cross the bilayer. When a 1.0 nm region around the center of the bilayer was searched for the presence of water molecules, 15 events were detected at pH 5.5 and 5 events were found at pH 7.0, while just 1 event was detected for the bilayer in the absence of peptides.

The activity of histidine-rich peptides was investigated in neutral and acidic conditions, and the literature reports examples of peptides that are active in both conditions to differing extents or with different mechanisms of action.[5,7,8] JI, with only one histidine residue, showed significant pore-forming activity at both pHs, which is increased at acidic pH. MD simulations also

dx.doi.org/10.1021/bi5003585 | *Biochemistry* 2014, 53, 4857−4868

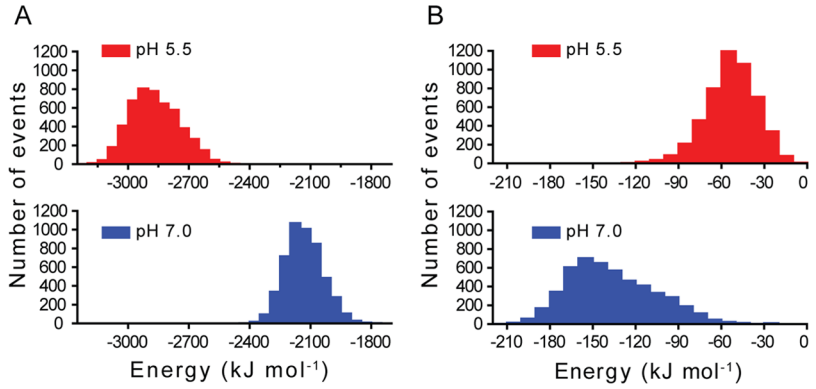

Figure 6. Influence of the protonation state of JI on its interaction with POPC/POPG 70:30 bilayer. Histograms of the Coulomb contribution to the interaction energy averaged over the last 50 ns of the simulation (A) between the peptides and the bilayer and (B) among the peptide molecules.

show increased activity in acidic conditions and suggest that a parallel alignment of peptide molecules in relation to the membrane plane prevails as was described for histidine-rich peptides.[7] However, no difference was detected in the alignment of peptides caused by the different pHs and no kind of pore involving JI could be detected, except for the passage of water molecules. The tendency of JI molecules to aggregate, which was verified in the simulations with 2, 4, and 16 molecules, may limit the peptide mobility,[33] either in water or in model membrane environments, and may have influenced or hindered its passage through the bilayer.

Effects of JI on Lipid Bilayer Characteristics. The anisotropy of the fluorescent probe DPH estimates the acyl chain order of lipid bilayers and reports the influence that the peptides may exert in this region. Figure 7C shows that in the absence of peptide the anisotropy of the bilayers increases in the order PC/PG 70:30 < PC/PS/Erg 40:40:20 < PC/SPH/Chol 40:40:20. *r*-Values around 0.2 have already been found for bilayers containing cholesterol, which indicates increased lipid packing and acyl chain order.[17] We observed that the presence of 20% ergosterol in PC/PS/Erg does not significantly increase the acyl chain order as 20% cholesterol does in the zwitterionic PC/SPH/Chol. Figure 7C also shows that increasing the concentration of JI does not influence *r*-value in LUVs of different composition. This finding indicates that JI interaction occurs in the region of the head groups of the phospholipids, as the MD results also indicated. Although peptides do not fully insert into the bilayer, Figure 7D shows that the order parameter (S_{CD}) of the saturated acyl chains increases in relation to the order parameter of the bilayer in the absence of peptides, except from carbon 2 to carbon 6. However, there is no significant difference between the order parameters obtained in the presence of peptides at pH 5.5 or 7.0. The average density profile of water, phosphate and some amino acid residues as a function of the distance to the bilayer center ($x = 0$) are exhibited in Figure 7E, comparing the influence of JI protonation state. It roughly reflects how different groups are positioned. The charged, polar residues and phenylalanine residues are in the phospholipid headgroup region and more deeply inserted in the bilayer at pH 5.5 than at pH 7.0.

CONCLUSIONS

Jelleines are among the shortest antimicrobial cationic peptides that are lytic to model membranes. A combined approach employing experiments of lytic activity and of the effects on model membranes with MD simulations was used to enhance our understanding of the factors that influence the peptide antimicrobial activity. MD simulations suggested that the Pro1 residue is probably the determinant of the strongest antimicrobial activity of JI in relation to the other natural jelleines. JI has preferential activity in anionic lipid bilayers over the zwitterionic ones. It binds to them and neutralizes part of their charges, showing stronger activity on bilayers with a more negative ζ potential. There is an apparent contradiction between intense leakage of PC/PG 70:30 vesicles and ζ potential values that level off at concentrations above 10 μM. Considering the tendency of JI to form aggregates as shown in MD simulations, its positive charges are not totally available to neutralization, but the accumulation can exert pressure on the surface and disturb the barrier characteristics of the bilayer, and leakage will continue to occur. The same behavior is seen with PC/PS/Erg 40:40:20 vesicles in ζ potential measurements. The lower threshold P/L in this *C. albicans* mimetic membrane could be attributed to its higher anionic character, but in the leveling off of JI lytic activity other influences might be at play, such as the differences in the electrostatic character of PS (two negative and one positive charge in the headgroup region) and the presence of ergosterol. JI has pore-forming activity that is enhanced at pH 5.5, at which it presents three positive charges due to the protonation of its histidine residue. From MD simulations, it is suggested that the Coulombic contribution to the interaction energy is more favorable at acidic pH and that this condition lowers the energy barrier for water passage through the bilayer.

The selective activity of JI toward anionic bilayers was already found in the short antimicrobial peptide anoplin. This peptide has four positively charged residues and exhibits poor CF leakage but very intense single channel activity[34] and exponential changes in ζ potential.[35] According to these features a toroidal pore-like mechanism was suggested.[34] In the present study, our findings point to a mechanism of action by which JI accumulates on the headgroup region of the vesicles before a significant leakage starts. Due to its tendency to aggregate and to remain in this form when interacting with POPC/POPG 70:30 bilayers, JI could exert pressure to accommodate its polar and nonpolar residues in the amphiphilic environment of the membrane. This pressure could open pores or defects, disturb the bilayer continuity, and allow the vesicle content to leak. The aggregated form of JI interaction with mimetic bilayers may have advantages and disadvantages to its efficiency as an antimicrobial peptide: the aggregated form increases local peptide concentration and may impair the proteolytic degradation; on the other hand, the

dx.doi.org/10.1021/bi5003585 | *Biochemistry* 2014, 53, 4857−4868

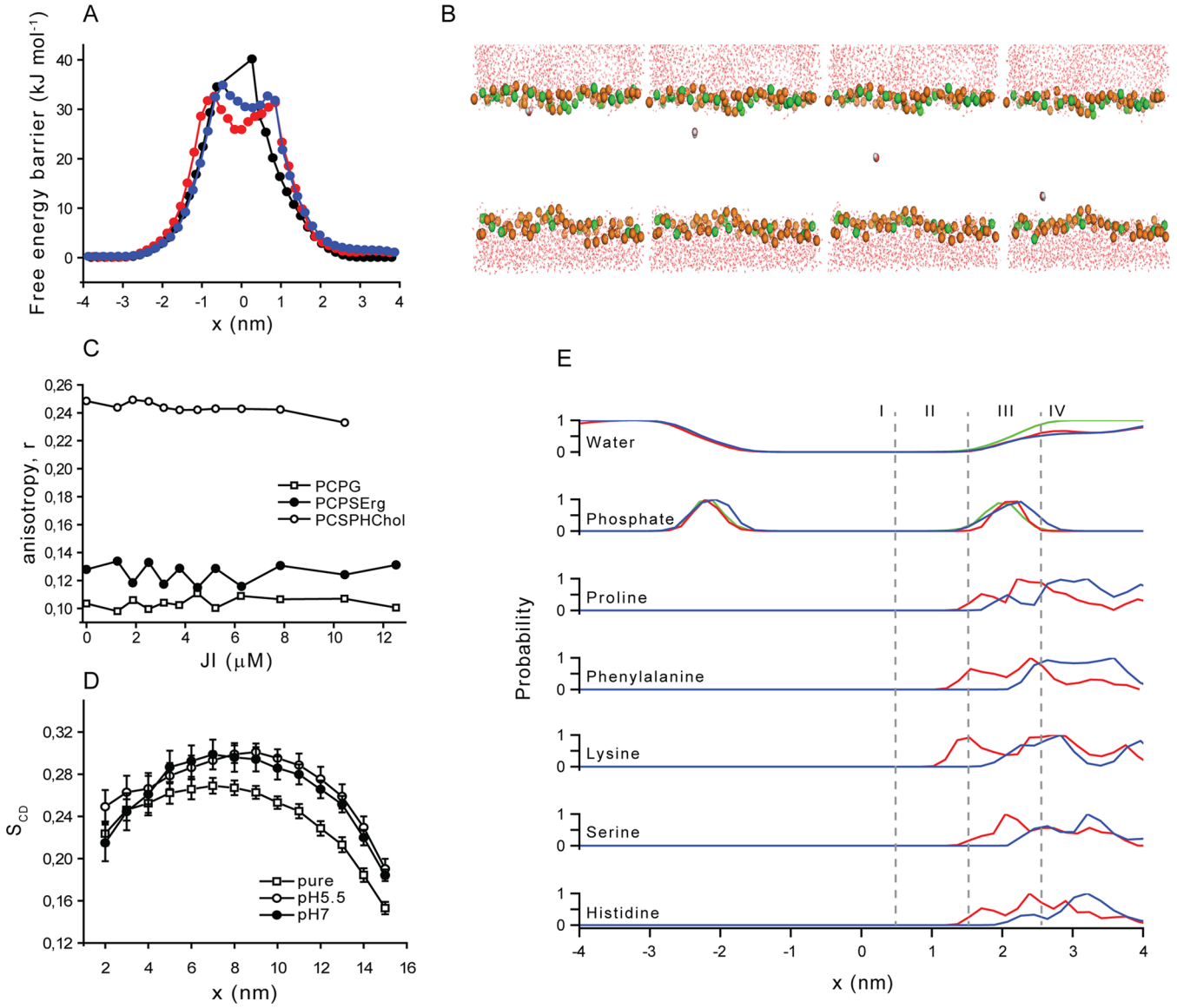

Figure 7. Effects of JI on the lipid bilayer characteristics. (A) The free energy barrier through the bilayer (black) in the absence of peptides, (blue) at pH 7.0, and (red) at pH 5.5. (B) A sequence of representative frames showing the passage of one water molecule. For clarity the phospholipid acyl chains and the water molecule crossing the acyl chain region were removed. Spheres represent POPC (orange) and POPG (green) head groups and oxygen of the water molecules (red). (C) Anisotropy of fluorescence emission, *r*, of the probe DPH (X = 0.002, excitation wavelength = 360 nm, emission wavelength = 450 nm) embedded in 50 μM LUVs, at pH 5.5 and at 25 °C. (D) Averaged order parameter (S_{CD}) of the saturated acyl-chains of the POPC/POPG 70:30 bilayer obtained from MD simulation in the absence of peptides (pure) and with 16 peptide molecules at pH 5.5 (open circle) and at pH 7.0 (filled circle). (E) Histograms of the probability of finding JI specific residues along the membrane normal at pH 5.5 (red) and at pH 7.0 (blue) and in the absence of peptides (green). From top to bottom: water, phosphate, proline, phenylalanine, lysine, serine, and histidine residues. For clarity the membrane is grouped into regions: (I) C10−C16 region; (II) C2−C9 region; (III) membrane−water interface; (IV) water region under the peptide influence.

nonaggregated form could be more efficient in neutralizing membrane charges.

■ ASSOCIATED CONTENT

Supporting Information

Experimental details on the peptide mass spectrometry analysis, vesicle preparation, and molecular dynamics simulations. Detailed results on the generation of the initial random configurations and on the influence of the protonated state of JI. This material is available free of charge via the Internet at http://pubs.acs.org.

■ AUTHOR INFORMATION

Corresponding Author

*Mailing address: Departamento de Química e Ciências Ambientais, IBILCE, UNESP, R. Cristóvão Colombo, 2265, 15054-000 São José do Rio Preto, SP, Brazil. Tel. 55-17-32212289. Fax 55-17-32212356. E-mail: cabrera.marcia@gmail.com (M.P.D.S.C.).

Funding

This work was supported in part by grants from Fundação de Amparo à Pesquisa do Estado de São Paulo (FAPESP), M.P.D.S.C. (2010/11823-0; 2012/24259-0) and M.A.-M. (2010/52077-9), and BIOprospecTA/FAPESP program

(Procs. 2006/57122-7 and 2011/51684-1, financing the synthesis of jelleines). L.C.S.-G. and G.B. are CNPq and Capes fellowship recipients, respectively.

Notes

The authors declare no competing financial interest.

■ ACKNOWLEDGMENTS

The authors are thankful to Prof. Dr. Marcio J. Tiera for the use of the laboratory infrastructure. M.S.P. is a researcher from the National Research Council of Brazil-CNPq. The authors also acknowledge the assistance of Dr. Deborah Capes from the Department of Medicine at the University of Wisconsin—Madison, USA, for the comments on the manuscript.

■ ABBREVIATIONS

JI, jelleine-I; POPC, palmitoyl-oleoyl-phosphatidylcholine; POPG, palmitoyl-oleoyl-phosphatidylglycerol; PC, egg phosphatidylcholine; PG, egg phosphatidylglycerol; Chol, cholesterol; Erg, ergosterol; SPH, sphingomyelin; PS, phosphatidyl-L-serine; SDS, sodium dodecyl sulfate; MD, molecular dynamics simulations; P/L, peptide to lipid molar ratio

■ REFERENCES

(1) Fabbretti, A., Gualerzi, C. O., and Brandi, L. (2011) How to cope with the quest for new antibiotics. *FEBS Lett. 585*, 1673−1681.

(2) Fontana, R., Mendes, M. A., de Souza, B. M., Konno, K., Cesar, L. M., Malaspina, O., and Palma, M. S. (2004) Jelleines: a family of antimicrobial peptides from the Royal Jelly of honeybees (*Apis mellifera*). *Peptides 25*, 919−928.

(3) Fontana, R. (2002) Caracterização molecular e functional de componentes antimicrobianos da geléia real de *Apis mellifera*. PhD thesis, pp 1−119, Universidade Estadual Paulista, Instituto de Biociencias de Rio Claro, SP, Brasil.

(4) Bechinger, B. (2011) Insights into the mechanisms of action of host defence peptides from biophysical and structural investigations. *J. Pept. Sci. 17*, 306−314.

(5) Kharidia, R., Tu, Z., Chen, L., and Liang, J. F. (2012) Activity and selectivity of histidine-containing lytic peptides to antibiotic-resistant bacteria. *Arch. Microbiol. 194*, 769−778.

(6) Makovitzki, A., and Shai, Y. (2005) pH-Dependent antifungal lipopeptides and their plausible mode of action. *Biochemistry 44*, 9775−9784.

(7) Kacprzyk, L., Rydengård, V., Mörgelin, M., Davoudi, M., Pasupuleti, M., Malmsten, M., and Schmidtchen, A. (2007) Antimicrobial activity of histidine-rich peptides is dependent on acidic conditions. *Biochim. Biophys. Acta 1768*, 2667−2680.

(8) Mason, A. J., Moussaoui, W., Abdelrahman, T., Boukhari, A., Bertani, P., Marquette, A., Shooshtarizaheh, P., Moulay, G., Boehm, N., Guerold, B., Sawers, R. J. H., Kichler, A., Metz-Boutigue, M.-H., Candolfi, E., Prévost, G., and Bechinger, B. (2009) Structural determinants of antimicrobial and antiplasmodial activity and selectivity in histidine-rich amphipathic cationic peptides. *J. Biol. Chem. 284*, 119−133.

(9) Makovitzki, A., Fink, A., and Shai, Y. (2009) Suppression of human solid tumor growth in mice by intratumor and systemic inoculation of histidine-rich and pH-dependent host defense−like lytic peptides. *Cancer Res. 69*, 3458−3463.

(10) Scocchi, M., Tossi, A., and Gennaro, R. (2011) Proline-rich antimicrobial peptides: converging to a non-lytic mechanism of action. *Cell. Mol. Life Sci. 68*, 2317−2330.

(11) Matsuzaki, K., Sugishita, K., Fujii, N., and Miyajima, K. (1995) Molecular Basis for Membrane Selectivity of an Antimicrobial Peptide, Magainin 2. *Biochemistry 34*, 3423−3429.

(12) Lohner, K., and Prenner, E. J. (1999) Differential scanning calorimetry and X-ray diffraction studies of the specificity of the interaction of antimicrobial peptides with membrane-mimetic systems. *Biochim. Biophys. Acta 1462*, 141−156.

(13) Löffler, J., Einsele, H., Hebart, H., Schumacher, U., Hrastnik, C., and Daum, G. (2000) Phospholipid and sterol analysis of plasma membranes of azole-resistant *Candida albicans* strains. *FEMS Microbiol. Lett. 185*, 59−63.

(14) Lizenko, M. V., Regerand, T. I., Bakhirev, A. M., and Lizenko, E. I. (2011) Lipid Composition of Cells and Low-Density Lipoproteins in Blood Serum of Human and Some Vertebrate Species. *J. Evol. Biochem. Physiol. 47* (5), 428−437.

(15) De Souza, B. M., Mendes, M. A., Santos, L. D., Marques, M. R., Cesar, L. M., Almeida, R. N., Pagnocca, F. C., Konno, K., and Palma, M. S. (2005) Structural and functional characterization of two novel peptide toxins isolated from the venom of the social wasp *Polybia paulista*. *Peptides 26*, 2157−2164.

(16) Mueller, P., Rudin, H. T., Tien, T., and Wescott, W. C. (1963) Methods for the formation of single bimolecular lipid membranes in aqueous solutions. *J. Phys. Chem. 67*, 534−535.

(17) Zhao, H., Sood, R., Jutila, A., Bose, S., Fimland, G., Nissen-Meyer, J., and Kinnunen, P. K. J. (2006) Interaction of the antimicrobial peptide pheromone Plantaricin A with model membranes: implications for a novel mechanism of action. *Biochim. Biophys. Acta 1758*, 1461−1474.

(18) Berendsen, H. J. C., van der Spoel, D., and van Drunen, R. (1995) GROMACS: A message-passing parallel molecular dynamics implementation. *Comput. Phys. Commun. 91*, 43−56.

(19) Hess, B., Kutzner, C., van Der Spoel, D., and Lindahl, E. (2008) GROMACS 4: Algorithms for highly efficient, load-balanced, and scalable molecular simulation. *J. Chem. Theory Comput. 4*, 435−447.

(20) van Gunsteren, W. F., Billeter, S. R., Eising, A. A., Hünenberger, P. H., Krüger, P., Mark, A. E., Scott, W. R. P., Tironi, I. G. (1996) *Biomolecular Simulation: The GROMOS96 Manual and User Guide*, pp 1−1042, Vdf Hochschulverlag AG an der ETH Zürich, Zürich, Switzerland.

(21) van Gunsteren, W. F., Berendsen, H. J. C. (1987) *Groningen Molecular Simulation (GROMOS) Library Manual*, pp 1−221, Biomos, Groningen, The Netherlands.

(22) Sammalkorpi, M., Karttunen, M., and Haataja, M. (2007) Structural properties of ionic detergent aggregates: a large-scale molecular dynamics study of sodium dodecyl sulfate. *J. Phys. Chem. B 111*, 11722−11733.

(23) Berger, O., Edholm, O., and Jähning, F. (1997) Molecular dynamics simulations of a fluid bilayer of dipalmitoylphosphatidylcholine at full hydratation, constant pressure, and constant temperature. *Biophys. J. 72*, 2002−2013.

(24) Zagrovic, B., Gattin, Z., Lau, J. K., Huber, M., and van Gunsteren, W. F. (2008) Structure and dynamics of two beta-peptides in solution from molecular dynamics simulations validated against experiment. *Eur. Biophys. J. 37*, 903−912.

(25) Hansen, P. R. (2010) Jelleine-I analogues with improved antibacterial activity. In *Tales of Peptides. Proceedings of the 31st European Peptide Symposium. Copenhagen, Denmark. Sept. 5−9* (Lebl, M., Meldal,M., Jensen, K. J., Hoeg-Jensen, T., Eds.), pp 376−377, European Peptide Society: San Diego, USA.

(26) Romanelli, A., Moggio, L., Montella, R. C., Campiglia, P., Iannaccone, M., Capuano, F., Pedone, C., and Capparelli, R. (2011) Peptides from royal jelly: studies on the antimicrobial activity of jelleins, jelleins analogs and synergy with temporins. *J. Pept. Sci. 17*, 348−352.

(27) Capparelli, R., De Chiara, F., Nocerino, N., Montella, R. C., Iannaccone, M., Fulgione, A., Romanelli, A., Avitabile, C., Blaiotta, G., and Capuano, F. (2012) New perspectives for natural antimicrobial peptides: Application as antinflammatory drugs in a murine model. *BMC Immunol. 13*, 61−74.

(28) Lim, K., Chua, R. R. Y., Saravanan, R., Basu, A., Mishra, B., Tambyah, P. A., Ho, B., and Leong, S. S. J. (2013) Immobilization Studies of an Engineered Arginine−Tryptophan-Rich Peptide on a Silicone Surface with Antimicrobial and Antibiofilm Activity. *ACS Appl. Mater. Interfaces 5*, 6412−6422.

(29) Haney, E. F., Hunter, H. N., Matsuzaki, K., and Vogel, H. J. (2009) Solution NMR studies of amphibian antimicrobial peptides: linking structure to function? *Biochim. Biophys. Acta 1788*, 1639−1655.
(30) Nishida, M., Imura, Y., Yamamoto, M., Kobayashi, S., Yano, Y., and Matsuzaki, K. (2007) Interaction of a magainin-PGLa hybrid peptide with membranes: insight in the mechanism of synergism. *Biochemistry 49*, 14284−14290.
(31) Wheaten, S. A., Lakshmanan, A., and Almeida, P. F. (2013) Statistical analysis of peptide-induced graded and all-or-none fluxes in giant vesicles. *Biophys. J. 105*, 432−443.
(32) Jin, Y., Hammer, J., Pate, M., Zhang, Y., Zhu, F., Zmuda, E., and Blazyk, J. (2005) Antimicrobial activities and structures of two linear cationic peptide families with various amphipathic β-sheet and α-helical potentials. *Antimicrob. Agents Chemother. 49*, 4957−4964.
(33) Ciobanasu, C., Harms, E., and Kubitscheck, U. (2009) Cell-penetrating HIV1 TAT peptides float on model lipid bilayers. *Biochemistry 48*, 4728−4737.
(34) Dos Santos Cabrera, M. P., Arcisio-Miranda, M., Broggio Costa, S. T., Konno, K., Ruggiero, J. R., Procopio, J., and Ruggiero Neto, J. (2008) Study of the mechanism of action of anoplin, a helical antimicrobial decapeptide with ion channel-like activity, and the role of the amidated C-terminus. *J. Pept. Sci. 14*, 661−669.
(35) Dos Santos Cabrera, M. P., Arcisio-Miranda, M., da Costa, L. C., de Souza, B. M., Broggio Costa, S. T., Palma, M. S., Ruggiero Neto, J., and Procopio, J. (2009) Interactions of mast cell degranulating peptides with model membranes: a comparative biophysical study. *Arch. Biochem. Biophys. 486*, 1−11.